



Cite this: *Polym. Chem.*, 2021, **12**, 1086

# Make or break: Mg(II)- and Zn(II)-catalen complexes for PLA production and recycling of commodity polyesters†

Jack Payne,<sup>a</sup> Paul McKeown,<sup>b</sup> Oliver Driscoll,<sup>b</sup> Gabriele Kociok-Köhn,<sup>b</sup> Emma A. C. Emanuelsson<sup>c</sup> and Matthew D. Jones<sup>a,\*</sup>

Recently we reported a series of highly active Al(III)-complexes bearing a catalen ligand support for lactide polymerisation, observing unprecedented activity in the melt. Herein we report diversification of the metal to furnish a series of well-defined dimeric Zn(II)- and Mg(II)-complexes, which were fully characterised by X-ray crystallography and NMR spectroscopy. The production of biocompatible atactic PLA from *rac*-LA in solution and under industrially preferred solvent-free conditions was demonstrated, typically observing good activity and  $M_n$  control with a broad range of dispersities ( $D = 1.08$ – $2.04$ ). Mg(II)-Complexes were shown to facilitate the relatively mild methanolysis of PLA, achieving up to 64% conversion to Me-LA within 8 h at 80 °C in THF. Further kinetic analysis found [Mg(**1,3**)]<sub>2</sub> to have  $k_{app}$  values of  $0.628 \pm 0.0536$  (4 wt% cat. loading) and  $0.265 \pm 0.0193$  h<sup>-1</sup> (8 wt% cat. loading) respectively for the rate of consumption of PLA. Preliminary work extended polymer scope to PET from various sources, demonstrating catalyst versatility.

Received 30th October 2020,  
Accepted 23rd December 2020

DOI: 10.1039/d0py01519a

rsc.li/polymers

## Introduction

Inexpensive, lightweight and robust, plastics remain a tremendous source of social and economic value, providing 1.6 million jobs and turning over € 360 billion in 2018 in Europe alone.<sup>1,2</sup> However, the current plastics economy remains fundamentally limited, dominated by petroleum-based products operating within a linear model, which underpins mounting environmental concerns.<sup>3–8</sup> Ocean plastics typify the severity of current plastic pollution with the Great Pacific Garbage Patch (GPGB), an accumulation zone of ocean plastics, encompassing *ca.* 1.6 million km<sup>2</sup>, equivalent to three times the area of France.<sup>9</sup> This has stimulated considerable research into renewable and environmentally friendly alternatives, for example poly(lactic acid) (PLA). Traditionally produced from the metal-mediated ring-opening polymerisation (ROP) of lactide (LA), a bio-based monomer feedstock, PLA has

subsequently found commercial use in both the packaging and biomedical sector.<sup>3,10–14</sup> Recent research has primarily sought to address toxicity concerns associated with the industry standard, Sn(Oct)<sub>2</sub>, through the development of biocompatible and environmentally benign alternatives.<sup>15–17</sup> Consequently, a diverse range of metals have been explored, including Al(III)<sup>18–35</sup> and group(IV),<sup>36–49</sup> with a particular focus on retaining activity whilst maintaining stereocontrol. Metals most pertinent to this report include Zn(II) and Mg(II), which are cheap and non-toxic. Zinc complexes have previously been shown to be highly effective initiators for the ROP of LA, generally observing high activity in solution.<sup>50–64</sup> Pioneering work by Coates and co-workers reported a highly heteroselective Zn(II)-complex bearing a  $\beta$ -diiminate ligand, achieving up to  $P_r = 0.94$  in the ROP of *rac*-LA at 0 °C.<sup>65</sup> Dizinc catalysts supported by macrocyclic ligands developed by Williams and co-workers remain the fastest reported to date under solution conditions, exhibiting high TOFs (up to 60 000 h<sup>-1</sup>) at room temperature in THF.<sup>66</sup> The most isoselective Zn(II)-complex known is an aminophenolate initiator reported by Ma and co-workers, which achieved  $P_r = 0.07$  at –40 °C.<sup>67</sup> McKeown *et al.*<sup>68</sup> have reported a series of simple Zn(II)-Schiff Base complexes capable of achieving TOFs in excess of 100 000 h<sup>-1</sup> under immortal conditions in the melt. Recently, Hermann *et al.*<sup>69</sup> reported a highly active and robust zinc-guanidine complex capable of producing colourless, high molecular weight ( $M_n \sim 150\,000$  g mol<sup>-1</sup>) PLA within minutes under solvent-free

<sup>a</sup>Centre for Sustainable and Circular Technologies, University of Bath, Claverton Down, Bath, BA2 7AY, UK

<sup>b</sup>Department of Chemistry, University of Bath, Claverton Down, Bath, BA2 7AY, UK.  
E-mail: mj205@bath.ac.uk

<sup>c</sup>Department of Chemical Engineering, University of Bath, Claverton Down, Bath, BA2 7AY, UK

† Electronic supplementary information (ESI) available: Full details of the experimental protocols with selected spectra and raw data. CCDC 2041361–2041367. For ESI and crystallographic data in CIF or other electronic format see DOI: 10.1039/d0py01519a

conditions ( $k_p = 1.43 \pm 0.09 \text{ L mol}^{-1} \text{ s}^{-1}$ ), culminating in the fastest reported system to date, significantly outperforming Sn(Oct)<sub>2</sub>. Magnesium complexes have also received significant interest in the ROP of LA.<sup>70–82</sup> Chisholm and co-workers have reported numerous Mg(II)-complexes for the production of heterotactic PLA ( $P_r = 0.90\text{--}0.96$ ).<sup>51,83–85</sup> Both Coates *et al.*<sup>50</sup> (Zn(II),  $P_r = 0.94$ ; Mg(II), atactic PLA) and Ma *et al.*<sup>58</sup> (Zn(II),  $P_r = 0.20$ ; Mg(II),  $P_r = 0.81$ ) have previously shown metal exchange to dramatically impact stereocontrol. Despite such promising advancements, the widespread use of PLA remains limited by a high production cost.<sup>3,11</sup> Additionally, if not disposed of appropriately, PLA is a potential contributor to the plastic waste crisis.<sup>3,86</sup> Plastic pollution mitigation requires the industry adopts a circular model, one concerned with material recapture and reuse, with recycling a potential solution.<sup>1,3,7</sup> Whilst mechanical recycling is traditionally employed, its long-term suitability is limited by eventual material downcycling.<sup>2,87</sup> A possible alternative is chemical recycling, which enables value-added products such as lactate esters, lactic acid and acrylic acid to be accessed.<sup>3,88,89</sup> Lactic acid has been identified as a platform chemical, whilst lactate esters have been cited as potential green solvent replacements owing to their low toxicity and biodegradability.<sup>90–93</sup> It is anticipated the potential for enhanced socio-economic performance will drive market penetration and reduce PLA production costs.<sup>94</sup> Indeed, the ethyl lactate market is projected to reach \$ 92 million by 2024 and currently trades at £ 2.54–3.49 per kg relative to £ 1.69 per kg for virgin PLA.<sup>91,95</sup> PLA recycling processes include hydrolysis<sup>96–103</sup> and alcoholysis.<sup>104–115</sup> Hydrogenation<sup>116–118</sup> and hydrosilylation<sup>119</sup> processes exploiting ruthenium and iridium have also been reported. Simple, commercially available metal salts and precursors (*e.g.* FeCl<sub>3</sub>) have been shown to facilitate the transesterification of PLA, typically in the presence of methanol to afford methyl lactate (Me-LA).<sup>120–122</sup> Sobota and co-workers demonstrated the transesterification of PLA using a wide range of alcohols in the presence of Mg(II) and Ca(II) pre-catalysts, typically operating under high temperature and pressure regimes.<sup>111</sup> Organocatalysts have also been exploited in PLA degradation, for example triazabicyclodecene (TBD), 4-(dimethylamino)pyridine (DMAP) and tetramethylammonium methyl carbonate.<sup>112–114</sup> McKeown *et al.*<sup>123</sup> recently demonstrated a homoleptic Zn(II)-complex bearing a propylenediamine backbone to be highly active for PLA methanolysis, achieving 84% conversion to Me-LA ( $Y_{\text{Me-LA}}$ ) within 1 h at 50 °C. The corresponding ethylenediamine analogue exhibited significantly reduced activity ( $Y_{\text{Me-LA}} = 12\%$  in 6 h) under comparable conditions (40 °C), highlighting the importance of structure-activity relationships.<sup>109,123</sup> However, the use of metal-based catalysts for this purpose remains rare despite the plethora reported for LA polymerisation. There is also a clear appetite to diversify metal scope to address potential long-term availability concerns associated with zinc.<sup>124</sup>

We recently reported a series of highly active Al(III)-complexes supported by a catalen framework for lactide polymerisation, observing unprecedented activity in the melt.<sup>35</sup> However, these complexes are inactive for PLA methanolysis.

Herein, we report diversification of the metal to Zn(II) and Mg(II) in pursuit of catalysts active for PLA degradation, for which there is existing literature precedent.<sup>109,111,123</sup> Consequently, a range of well-defined dimeric Zn(II)- and Mg(II)-catalen complexes were prepared, employing a new and emerging class of ligands in the area. Their application to the ROP of *rac*-LA in solution, and under industrially preferred melt conditions, is discussed. The relatively mild metal-mediated methanolysis of PLA into Me-LA is reported. Preliminary work diversifying polyester scope is also demonstrated.

## Results and discussion

### Synthesis

The catalen ligands were prepared *via* a simple two-step synthesis (Scheme 1), exploiting successive condensation reactions, and characterised by <sup>1</sup>H NMR spectroscopy and mass spectrometry (MS). <sup>1</sup>H NMR spectroscopic analysis revealed a characteristic singlet at *ca.*  $\delta = 8.40$  ppm, corresponding to a HC=N resonance, confirming formation of the imine. The –CH<sub>2</sub> resonances were observed as two distinct triplets between *ca.*  $\delta = 3.40$  and 3.80 ppm. Dimeric complexes of Zn(II) and Mg(II) were then prepared in anhydrous toluene and recrystallised from the reaction solvent (Scheme 1). All complexes were characterised by single crystal X-ray diffraction (XRD) as shown in Fig. 1. Selected bond lengths and angles for [Zn(1–3)]<sub>2</sub> and [Mg(1–3)]<sub>2</sub> are provided in the ESI.† A Zn(1)–N(2) and Mg(1)–N(2) bond length of *ca.* 2 Å confirmed retention of the imine functionality present in 1–3H<sub>2</sub> upon coordination to the metal centre. In all instances,  $\tau_5$  values tended towards 1, indicative of a distorted trigonal bipyramidal geometry (see ESI†). Interestingly, a highly unusual tetrameric Mg(II)-complex based on an amine-deprotonated derivative of 2H<sub>2</sub> was isolated and characterised by XRD (Fig. 2). Direct concentration of the same solution led to the isolation of [Mg(2)]<sub>2</sub> in good purity. The tetramer exhibited an Mg(1)–N(1) bond length of *ca.* 0.20 Å shorter relative to [Mg(2)]<sub>2</sub> as expected {Mg(1)–N(1): tetramer, 2.078(4); [Mg(2)]<sub>2</sub>, 2.2181(19)}. Tetrameric analogues based on 1,3H<sub>2</sub> and Zn(II) were not



**Scheme 1** Catalen ligand preparation and subsequently derived Zn(II)- and Mg(II)-complexes.





Fig. 1 Solid-state structures of  $[\text{Zn}(\mathbf{1-3})]_2$  (top left to right) and  $[\text{Mg}(\mathbf{1-3})]_2$  (bottom left to right). Ellipsoids shown at 30% probability with the exception of  $[\text{Mg}(\mathbf{2})]_2$ , which is shown at 50% probability. All hydrogen atoms except those bound to nitrogen or involved in hydrogen bonding, as noted for  $[\text{Mg}(\mathbf{2-3})]_2$ , have been omitted for clarity.

observed, whilst synthesis reattempts were unsuccessful.  $^1\text{H}$  NMR spectroscopic analysis of  $[\text{Zn}(\mathbf{1-3})]_2$  and  $[\text{Mg}(\mathbf{1-3})]_2$  revealed characteristic singlets at *ca.*  $\delta = 8.00$  and  $4.50$  ppm

corresponding to ArCHN and  $-\text{NH}$  resonances respectively. More interestingly, diastereotopic  $-\text{CH}_2$  resonances between *ca.*  $\delta = 3.50$  and  $4.00$  ppm were observed, indicating the ligand is locked in position once coordinated (see ESI†).  $^{13}\text{C}\{^1\text{H}\}$  NMR spectroscopic analysis was consistent with  $^1\text{H}$  NMR and XRD analysis. It is proposed the dimeric structure observed in the solid-state is retained in solution.  $\text{Zn}(\text{II})$ - and  $\text{Mg}(\text{II})$ -complexes were in generally good agreement with elemental analysis (EA) data obtained, demonstrating their purity. However, C% values were consistently low on  $[\text{Mg}(\mathbf{2-3})]_2$ , potentially due to air and moisture sensitivity confounded by high hygroscopicity, consistent with the  $\text{Al}(\text{III})$ -catalens.<sup>35</sup>

### Polymerisation of *rac*-LA

All  $\text{Zn}(\text{II})$ - and  $\text{Mg}(\text{II})$ -complexes were trialled in the ROP of *rac*-LA under solvent-free conditions (130 and 180 °C) in alignment with industrial practices (Table 1). Industrially, solvents are a significant source of waste and thus catalysts that operate under melt conditions are highly desirable.<sup>3,15,68,69</sup> All initiators were also tested out under solution conditions (80 °C) (Table 2). The lactide monomer, *rac*-LA, was recrystallised from anhydrous toluene once prior to use and benzyl alcohol (BnOH) was employed as a co-initiator. Conversion was determined *via* analysis of the methine region (*ca.*  $\delta = 4.9$ – $5.2$  ppm) using  $^1\text{H}$  NMR spectroscopy. To ensure one



Fig. 2 Solid-state structure of a tetrameric  $\text{Mg}(\text{II})$ -complex based on an amine-deprotonated derivative of  $2\text{H}_2$ . Ellipsoids shown at 30% probability. All hydrogen atoms and methyl groups of the  $t\text{Bu}$  groups have been omitted for clarity.



**Table 1** Melt polymerisation of *rac*-LA using [Zn(1-3)]<sub>2</sub> and [Mg(1,3)]<sub>2</sub>

Init.	Time/min	[ <i>rac</i> -LA]:[M]:[BnOH]	Conv. <sup>a</sup> /%	<i>M</i> <sub>n,theo</sub> <sup>b</sup> /g mol <sup>-1</sup>	<i>M</i> <sub>n</sub> <sup>c</sup> /g mol <sup>-1</sup>	<i>D</i> <sup>c</sup>	<i>P</i> <sub>r</sub> <sup>d</sup>
[Zn(1)] <sub>2</sub>	20	300 : 1 : 1	69	29 900	28 600	1.37	0.57
	90	3000 : 1 : 10	68	29 500	23 500	2.04	0.53
[Zn(2)] <sub>2</sub>	17	300 : 1 : 1	63	27 300	21 600	1.24	0.54
	60	3000 : 1 : 10	69	29 900	25 150	1.58	0.52
[Zn(3)] <sub>2</sub>	16	300 : 1 : 1	69	29 900	23 050	1.37	0.57
	50	3000 : 1 : 10	60	26 000	22 750	1.91	0.52
[Mg(1)] <sub>2</sub>	20 <sup>e</sup>	300 : 1 : 1	69	29 900	—	—	—
	120	3000 : 1 : 10	64	27 750	8750	1.58	0.49
[Mg(3)] <sub>2</sub>	8	300 : 1 : 1	71	30 800	17 900	1.50	0.54
	70	3000 : 1 : 10	69	29 900	16 800	2.00	0.50

Reaction conditions: *rac*-LA (1.0 g), solvent-free (130 °C). <sup>a</sup> Determined *via* <sup>1</sup>H NMR spectroscopy. <sup>b</sup> Theoretical average number molecular weight (*M*<sub>n</sub>) dependent on conversion and co-initiator added {(*M*<sub>rac-LA</sub> × 3 × %<sub>conv</sub>) + *M*<sub>n,BnOH</sub>}. <sup>c</sup> Determined *via* GPC analysis (in THF). <sup>d</sup> Determined *via* homonuclear decoupled NMR spectroscopy. <sup>e</sup> Insufficient polymeric material isolated for material characterisation. N.B. {[*rac*-LA]:[M]:[BnOH] = 3000 : 1 : 10} were performed at 180 °C. [M]:[BnOH] = 1 : 1 corresponds to 1 equivalent of BnOH per metal centre. Monomer conversion plateau between 60–70% can be attributed to reduced catalyst activity coupled with mass transfer limitations.

**Table 2** Solution polymerisation of *rac*-LA using [Zn(1-3)]<sub>2</sub> and [Mg(1,3)]<sub>2</sub>

Init.	Time/h	[ <i>rac</i> -LA]:[M]:[BnOH]	Conv. <sup>a</sup> /%	<i>M</i> <sub>n,theo</sub> <sup>b</sup> /g mol <sup>-1</sup>	<i>M</i> <sub>n</sub> <sup>c</sup> /g mol <sup>-1</sup>	<i>D</i> <sup>c</sup>	<i>P</i> <sub>r</sub> <sup>d</sup>
[Zn(1)] <sub>2</sub>	8	100 : 1 : 1	60	8750	124 00 <sup>e</sup>	1.08 <sup>e</sup>	0.61
[Zn(2)] <sub>2</sub>	8 <sup>f</sup>	100 : 1 : 1	31	4550	—	—	—
[Zn(3)] <sub>2</sub>	8 <sup>f</sup>	100 : 1 : 1	21	3150	—	—	—
[Mg(1)] <sub>2</sub>	1.5	100 : 1 : 1	94	13 650	13 900	1.17	0.46
[Mg(3)] <sub>2</sub>	8	100 : 1 : 1	77	12 000	9400	1.63	0.48

Reaction conditions: *rac*-LA (0.5 g), solvent (toluene, 80 °C). <sup>a</sup> Determined *via* <sup>1</sup>H NMR spectroscopy. <sup>b</sup> Theoretical average number molecular weight (*M*<sub>n</sub>) dependent on conversion and co-initiator added {(*M*<sub>rac-LA</sub> × %<sub>conv</sub>) + *M*<sub>n,BnOH</sub>}. <sup>c</sup> Determined *via* GPC analysis (in THF). <sup>d</sup> Determined *via* homonuclear decoupled NMR spectroscopy. <sup>e</sup> Bimodal GPC observed, distributions treated together for reported *M*<sub>n</sub> and *D* values. <sup>f</sup> Insufficient polymeric material isolated for material characterisation. N.B. [M]:[BnOH] = 1 : 1 corresponds to 1 equivalent of BnOH per metal centre.

–OBn moiety was associated per metal centre, both Zn(II)- and Mg(II)-complexes were treated as monomeric. It is proposed [Zn(1-3)]<sub>2</sub> and [Mg(1-3)]<sub>2</sub> operate *via* an activated-monomer mechanism. To investigate this the stability of [Zn(1)]<sub>2</sub> with excess BnOH was studied using <sup>1</sup>H NMR (CDCl<sub>3</sub>), which confirmed [Zn(1)]<sub>2</sub> to be stable at both room temperature and 80 °C (see ESI†). Due to a poor isolation yield (0.065 g, 14%), [Mg(2)]<sub>2</sub> was not pursued in polymerisation studies but was expected to exhibit comparable activity to [Mg(3)]<sub>2</sub> based on previous work.<sup>35</sup>

All Zn(II)-complexes exhibited good activity at 130 °C, achieving reasonably high conversion within 20 minutes {[*rac*-LA]:[M]:[BnOH] = 300 : 1 : 1} (Table 1). [Zn(2-3)]<sub>2</sub> exhibited superior activity relative to [Zn(1)]<sub>2</sub>, presumably owing to a more Lewis acid Zn(II)-centre. [Zn(1)]<sub>2</sub> exhibited excellent *M*<sub>n</sub> control (*M*<sub>n,theo</sub> = 29 900 g mol<sup>-1</sup>, *M*<sub>n</sub> = 28 600 g mol<sup>-1</sup>; Table 1, entry 1), whilst reasonable *M*<sub>n</sub> control was maintained for [Zn(2-3)]<sub>2</sub>, observing moderate dispersities (*D* = 1.24–1.37) in all cases. Reducing the catalyst loading to 0.033 mol% at 180 °C to simulate industrial conditions resulted in prolonged polymerisation times, achieving between 60–69% within 50 to 90 minutes {[*rac*-LA]:[M]:[BnOH] = 3000 : 1 : 10} (Table 1). The reactivity trend noted for [Zn(1-3)]<sub>2</sub> was exacerbated under these conditions, likely due to an increase in temperature

assisting catalyst dissociation and solubility. Interestingly, [Zn(1)]<sub>2</sub> exhibited poorer *M*<sub>n</sub> control (*M*<sub>n,theo</sub> = 29 500 g mol<sup>-1</sup>, *M*<sub>n</sub> = 23 500 g mol<sup>-1</sup>; Table 1, entry 2), whilst comparable control was retained for [Zn(2-3)]<sub>2</sub> under these conditions. Generally, a lower *M*<sub>n</sub> value than expected (relative to theoretical values) was observed, possibly indicative of side transesterification reactions, consistent with the broader dispersities observed (*D* = 1.58–2.04). Reactivity trends discussed for [Zn(1-3)]<sub>2</sub> could be extended to the Mg(II)-catalen series, observing comparable activity between [Zn(1)]<sub>2</sub> and [Mg(1)]<sub>2</sub> at 130 °C (Table 1). Both [Mg(1,3)]<sub>2</sub> exhibited reduced activity relative to their Zn(II) counterparts at 180 °C, suggesting the active species to be inherently less active, despite [Mg(3)]<sub>2</sub> (71%, 8 min; Table 1, entry 9) outperforming [Zn(3)]<sub>2</sub> (69%, 16 min; Table 1, entry 5) at 130 °C. However, significantly lower *M*<sub>n</sub> values relative to those reported for the Al(III)-catalens (*M*<sub>n</sub> = 160 500–252 100 g mol<sup>-1</sup>) were observed, implying *k*<sub>p</sub> to be significantly slower relative to *k*<sub>i</sub>, possibly due to a mechanism shift. Under both sets of conditions, [Mg(1,3)]<sub>2</sub> exhibited poor *M*<sub>n</sub> control (*M*<sub>n,theo</sub> = 27 750–30 800 g mol<sup>-1</sup>, *M*<sub>n</sub> = 8750–17 900 g mol<sup>-1</sup>). MALDI-ToF analysis confirmed the polymer (Table 1, entry 8) to be –OBn and –H end-capped with multiple series present indicating a high degree of transesterification (see ESI†), consistent with the broad dispersities





observed ( $\bar{D} = 1.50\text{--}2.00$ ). Metal exchange was found to have no impact on stereocontrol, observing the production of atactic PLA in all instances ( $P_r = 0.49\text{--}0.57$ ).

Under solution conditions  $\{[rac\text{-LA}]:[M]:[BnOH] = 100:1:1\}$  (Table 2),  $[Zn(1)]_2$  exhibited good polymerisation control, producing PLA of reasonably well-defined  $M_n$  ( $M_{n,theo} = 8750\text{ g mol}^{-1}$ ,  $M_n = 12\,400\text{ g mol}^{-1}$ ; Table 2, entry 1) and narrow dispersities ( $\bar{D} = 1.08$ ). GPC analysis revealed the  $M_n$  distribution to be bimodal in nature (see ESI†). Surprisingly,  $[Zn(2\text{--}3)]_2$  exhibited poorer activity relative to  $[Zn(1)]_2$ , achieving between 21–31% conversion within 8 h, contrary to reactivity trends discussed for the melt (Table 1). This activity loss could potentially be due to greater catalyst aggregation under these conditions, which limits availability of the active species. Indeed, kinetically limited dissociation was previously reported for the Al(III)-catalens, resulting in a loss in polymerisation control.<sup>35</sup> This trend was reflected in the Mg(II)-series but appeared less prevalent, consistent with observations in the melt. Promisingly, both  $[Mg(1,3)]_2$  outperformed their Zn(II) counterpart, achieving 94% and 77% conversion within 1.5 and 8 h respectively. MALDI-ToF analysis confirmed polymer produced by  $[Mg(3)]_2$  (Table 2, entry 5) to be  $-OBn$  and  $-H$  end-capped and transesterified, consistent with GPC analysis ( $M_{n,theo} = 12\,000\text{ g mol}^{-1}$ ,  $M_n = 9400\text{ g mol}^{-1}$ ,  $\bar{D} = 1.63$ ; Table 2, entry 5) (see ESI†). Interestingly,  $[Mg(1)]_2$  also facilitated intermolecular transesterification, consistent with a  $72\text{ g mol}^{-1}$  peak separation in the MALDI-ToF spectra (see ESI†), but maintained excellent polymerisation control ( $M_{n,theo} = 13\,650\text{ g mol}^{-1}$ ,  $M_n = 13\,900\text{ g mol}^{-1}$ ,  $\bar{D} = 1.17$ ; Table 2, entry 4). It is possible transesterification was exacerbated during polymer work up in the presence of MeOH, consistent with the melt (Table 1, entries 7–10).  $[Mg(1,3)]_2$  produced atactic polymer ( $P_r = 0.46\text{--}0.48$ ), whilst  $[Zn(1)]_2$  afforded PLA with a slight heterotactic bias ( $P_r = 0.61$ ). In summary, all Zn(II)- and Mg(II)-complexes exhibited good activity in the production of biocompatible atactic PLA, although non-competitive with the industry standard; Sn(Oct)<sub>2</sub>.

### Polymerisation kinetics

To ascertain a better understanding of metal-ligand cooperative effects on activity, a kinetic study was pursued using  $[Zn(1)]_2$  and  $[Mg(1)]_2$  as a model system. A plot of  $\ln([LA]_0/[LA])$  against time exhibited a linear relationship, indicating the reaction to be pseudo-first-order with respect to the consumption of *rac*-LA (Fig. 3).  $[Mg(1)]_2$  exhibited an apparent rate constant ( $k_{app}$ ) of  $0.0206\text{ min}^{-1}$ , over 12 orders of magnitude higher relative to  $[Zn(1)]_2$  ( $k_{app} = 0.0017\text{ min}^{-1}$ ), consistent with solution results (Table 2). Indeed,  $[Zn(1)]_2$  also exhibited an induction period of *ca.* 40 minutes, potentially evidencing catalyst aggregation under these conditions. No induction period was observed for  $[Mg(1)]_2$ , highlighting judicious choice of the metal can circumvent such limitations. It is tentatively suggested such aggregation is H-bonding in nature, although metal influence remains poorly understood. GPC analysis of the aliquots retained for  $[Mg(1)]_2$  confirmed the polymerisation to be well controlled and living (Fig. 4). This was demon-

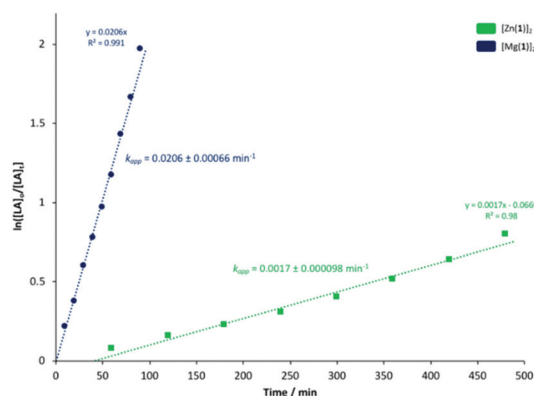


Fig. 3 Pseudo-first-order logarithmic plot for the polymerisation of *rac*-LA at 80 °C in toluene  $\{[rac\text{-LA}]:[M]:[BnOH] = 100:1:1\}$  using  $[Zn(1)]_2$  and  $[Mg(1)]_2$ . N.B.  $[LA]_0 = 0.69\text{ mol dm}^{-3}$ .



Fig. 4 Linear plot of  $M_n$  and  $\bar{D}$  against conversion for the polymerisation of *rac*-LA at 80 °C in toluene  $\{[rac\text{-LA}]:[M]:[BnOH] = 100:1:1\}$  using  $[Mg(1)]_2$ .

strated by a linear increase in  $M_n$  with conversion whilst maintaining narrow dispersities. A slightly lower  $M_{r,monomer}$  relative to ideal PLA was observed ( $M_{r,theo} = 144.12\text{ g mol}^{-1}$ ,  $M_r = 118.27\text{ g mol}^{-1}$ ), which could likely be attributed to minor transesterification, consistent with MALDI-ToF analysis (see ESI†).

### Polyester recycling

**PLA degradation.**  $[Zn(1\text{--}3)]_2$  and  $[Mg(1,3)]_2$  were investigated in the metal-mediated degradation of PLA into Me-LA in solution at 80 °C (Fig. 5 and Table 3). Whilst Me-LA is a possible green solvent replacement, it is also a potentially valuable chemical to the PLA supply chain since it can be directly converted to lactide.<sup>3,91</sup> Commercially available polymer (0.25 g, PLLA cup,  $M_n = 45\,510\text{ g mol}^{-1}$ ) and catalyst were dissolved in either THF or anhydrous toluene under Ar, with heat and stirring assisting dissolution. MeOH was then added and the conversion to Me-LA was determined *via*  $^1\text{H}$  NMR analysis of the methine region (*ca.*  $\delta = 4.2\text{--}5.2\text{ ppm}$ ). The production of Me-LA has previously been shown to proceed *via* a two-step process through the intermediate formation of chain-end groups (see ESI†).<sup>109,123</sup>



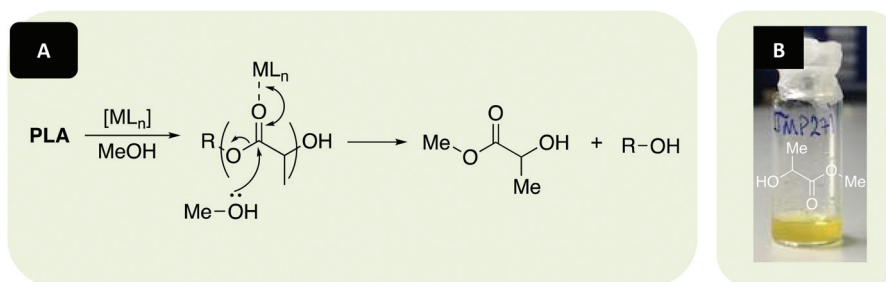


**Fig. 5** (A) Metal-mediated degradation mechanism of PLA into methyl lactate (Me-LA) via transesterification with MeOH, where R denotes the growth polymer chain. (B) Example of recycled product (Me-LA). N.B. Discolouration in Me-LA product (B, liquid) originates from catalyst used ( $[\text{Mg}(\mathbf{1})]_2$  – yellow solid).

**Table 3** Degradation of PLA into Me-LA using  $[\text{Zn}(\mathbf{1-3})_2]$  and  $[\text{Mg}(\mathbf{1,3})_2]$

Catalyst	Time/h	$T/^{\circ}\text{C}$	Cat. loading/wt%	$Y_{\text{Me-LA}}/\%$	$S_{\text{Me-LA}}/\%$	$X_{\text{int}}/\%$	$k_{\text{app}}/\text{h}^{-1}$
[Zn(1)] <sub>2</sub>	8	80	8	19	28	68	—
	8	80	4	4	9	46	—
	8 <sup>a</sup>	80	8	51	53	96	—
	8 <sup>a</sup>	80	4	7	12	57	—
[Zn(2)] <sub>2</sub>	8	80	8	0	0	42	—
	8	80	4	0	0	20	—
	8 <sup>a</sup>	80	8	4	9	44	—
	8 <sup>a</sup>	80	4	0	0	28	—
[Zn(3)] <sub>2</sub>	8	80	8	0	0	36	—
	8 <sup>a</sup>	80	8	0	0	37	—
[Mg(1)] <sub>2</sub>	8	80	2	10	36	28	—
	8	80	4	64	66	97	0.628
	8	80	8	31	56	55	0.0819
[Mg(3)] <sub>2</sub>	8	80	2	13	38	34	—
	8	80	4	42	63	67	—
	8	80	8	64	77	83	0.265

Reaction conditions: 0.25 g of PLLA cup ( $M_n = 45\,510\text{ g mol}^{-1}$ ),  $V_{\text{THF}}:V_{\text{MeOH}} = 4:1$ ,  $n_{\text{MeOH}}:n_{\text{ester}} = 7:1$ ,  $[\text{Zn(1-3)}]_2 = 4\text{--}8\text{ wt\% cat. loading}$  (0.24–0.58 mol% relative to ester linkages),  $[\text{Mg(1,3)}]_2 = 2\text{--}8\text{ wt\% cat. loading}$  (0.13–0.57 mol% relative to ester linkages).  $Y_{\text{Me-LA}}$ ,  $S_{\text{Me-LA}}$  and  $X_{\text{int}}$  determined by  $^1\text{H NMR}$  upon solvent removal. <sup>a</sup>Solvent: Anhydrous toluene,  $V_{\text{toluene}}:V_{\text{MeOH}} = 4:1$ .

Consequently, the methine groups can be categorised as internal (int), chain-end (CE) and those corresponding directly to the alkyl lactate (Me-LA). Conversion of internal methine units ( $X_{\text{int}}$ ), methyl lactate selectivity ( $S_{\text{Me-LA}}$ ) and Me-LA yield ( $Y_{\text{Me-LA}}$ ) are tabulated in Table 3 below.  $[\text{Zn}(\mathbf{1})]_2$  exhibited reasonably poor activity at 8 wt%, achieving 19% conversion to Me-LA within 8 h in THF with poor selectivity (Table 3, entry 1). Promisingly, superior activity and selectivity ( $Y_{\text{Me-LA}} = 51\%$ ,  $S_{\text{Me-LA}} = 53\%$ ,) was observed upon shifting to a non-coordinating solvent, namely anhydrous toluene (Table 3, entry 3). This implies THF competes with the degrading polymeric chain with respect to coordination to the Zn(II)-centre, consistent with the near complete consumption of PLA ( $X_{\text{int}} = 96\%$ ). Interestingly, shifting to a more electron withdrawing catalan backbone in  $[\text{Zn}(\mathbf{2-3})]_2$  had a detrimental impact on  $Y_{\text{Me-LA}}$ , achieving 0% conversion to Me-LA under analogous conditions in THF. Whilst contrary to previous work by Payne *et al.*,<sup>110</sup> this was consistent with solution polymerisation results (Table 2). Indeed, previously described solution reactivity trends were retained for PLA degradation. Since this behaviour was retained in anhydrous toluene, it is suggested the afore-

mentioned activity loss due to possible catalyst aggregation (Table 2) likely persists under these conditions. It is possible bulky <sup>t</sup>Bu substituents promote the dissociation of [Zn(1)<sub>2</sub>] in solution, resulting in superior activity relative to [Zn(2-3)<sub>2</sub>]. [Mg(1)<sub>2</sub>] significantly outperformed its Zn(II)-counterpart, achieving 31% conversion to Me-LA with good selectivity in THF at 8 wt% (Table 3, entry 13). Interestingly, significantly enhanced activity was realised upon decreasing the catalyst loading to 4 wt% (*Y*<sub>Me-LA</sub> = 64%, *S*<sub>Me-LA</sub> = 66%, *X*<sub>int</sub> = 97%), possibly evidencing a reduction in catalyst aggregation due to dilution. To improve industrial feasibility and investigate the limit of this effect, the catalyst loading was further reduced to 2 wt%. Significantly reduced *Y*<sub>Me-LA</sub> relative to 4 wt% was observed (Table 3, entries 11 and 12), implying unavailability of the active species predominates, consistent with [Mg(3)<sub>2</sub>] (Table 3, entry 14). In light of this, [Zn(1-3)<sub>2</sub>] were investigated at 4 wt% in both THF and anhydrous toluene at 80 °C, although no activity enhancement was observed. [Mg(3)<sub>2</sub>] exhibited superior activity relative to [Zn(3)<sub>2</sub>], achieving 42% conversion to Me-LA within 8 h at 4 wt% (Table 3, entry 15). Whilst lower relative to [Mg(1)<sub>2</sub>], enhanced *Y*<sub>Me-LA</sub> and *S*<sub>Me-LA</sub>

was observed at 8 wt% (Table 3, entry 16). This implies the liberated species to be inherently more active relative to  $[\text{Mg}(\text{1})]_2$  and that possible catalyst aggregation dominates at 4 wt%. Judicial choice of the metal had previously been shown to circumvent such challenges in the solution polymerisation of *rac*-LA (Fig. 3). Degradation reactions using  $[\text{Mg}(\text{1,3})]_2$  in anhydrous toluene were not pursued in alignment with the 12 principles of green chemistry.<sup>125</sup> Overall, mass transfer limitations due to polymer particle size and stirring speeds were considered negligible based on previous work by Román-Ramírez *et al.*,<sup>109</sup> which employed a homoleptic  $\text{Zn}(\text{II})$ -complex bearing an ethylenediamine Schiff-base ligand.

**PLA degradation kinetics.**  $[\text{Mg}(\text{1})]_2$  and  $[\text{Mg}(\text{3})]_2$  were identified as the outstanding candidates and thus pursued for further kinetic analysis. Reaction progress was monitored hourly for the first 4 hours for  $^1\text{H}$  NMR ( $\text{CDCl}_3$ ) analysis of the methine region. A final aliquot was taken after 8 hours for analysis, totalling 5 data points (Fig. 6). PLA consumption was assumed to adopt pseudo-first-order kinetics in accordance to previous work by Román-Ramírez *et al.*<sup>109</sup> Consequently, the gradient of the logarithmic plot is equivalent to the apparent rate constant,  $k_{\text{app}}$  (Table 3 and Fig. 6).  $[\text{Mg}(\text{1})]_2$  exhibited a  $k_{\text{app}}$  value of  $0.628 \pm 0.0536$  and  $0.0819 \pm 0.0213 \text{ h}^{-1}$  at 4 and 8 wt% respectively in THF, indicating an increase in catalyst loading results in a statistically significant decrease in activity.  $[\text{Mg}(\text{3})]_2$  was found to have a  $k_{\text{app}}$  value of  $0.265 \pm 0.0193 \text{ h}^{-1}$ , lower relative to  $[\text{Mg}(\text{1})]_2$ , consistent with preliminary methanolysis results (Table 3). Comparable  $Y_{\text{Me-LA}}$  values (Table 4) were observed relative to Table 3, indicating good reproducibility. Whilst promising, these  $k_{\text{app}}$  value remain lower compared to previously reported  $\text{Zn}(\text{II})$ -complexes ( $k_{\text{app}} = 0.44\text{--}12.0 \text{ h}^{-1}$ ) operating between 50 to 80 °C under analogous reaction conditions.<sup>109,110,123</sup> However, to the best of our knowledge,  $[\text{Mg}(\text{1,3})]_2$  represent the first example of PLA methanolysis mediated by a well-defined discrete  $\text{Mg}(\text{II})$ -complex, operating under significantly milder conditions relative to Petrus *et al.*,<sup>111</sup> who relied upon metallic Mg or  $\text{Mg}(\text{nBu})_2$  as pre-catalysts. For  $[\text{Mg}(\text{1,3})]_2$ , inspection of the  $^1\text{H}$  NMR (Table 3,

**Table 4** PLLA cup degradation using  $[\text{Mg}(\text{1,3})]_2$  in THF at 80 °C

Catalyst	$Y_{\text{Me-LA}}/\%$	$k_{\text{app}}/\text{h}^{-1}$
$[\text{Mg}(\text{1})]_2^a$	76	$0.628 \pm 0.0536$
$[\text{Mg}(\text{1})]_2^b$	38	$0.0819 \pm 0.0213$
$[\text{Mg}(\text{3})]_2^c$	63	$0.265 \pm 0.0193$

Reaction conditions: 0.25 g of PLLA cup ( $M_n = 45\,510 \text{ g mol}^{-1}$ ),  $V_{\text{THF}}:V_{\text{MeOH}} = 4:1$ ,  $n_{\text{MeOH}}:n_{\text{ester}} = 7:1$ . Error associated with  $k_{\text{app}}$  calculated using linear regression. <sup>a</sup> $[\text{Mg}(\text{1})]_2 = 4 \text{ wt\% cat. loading}$  (0.29 mol% relative to ester linkages). <sup>b</sup> $[\text{Mg}(\text{1})]_2 = 8 \text{ wt\% cat. loading}$  (0.57 mol% relative to ester linkages). <sup>c</sup> $[\text{Mg}(\text{3})]_2 = 8 \text{ wt\% cat. loading}$  (0.53 mol% relative to ester linkages). N.B.  $Y_{\text{Me-LA}}$  refers to maximum Me-LA conversion determined *via*  $^1\text{H}$  NMR ( $\text{CDCl}_3$ ) after 8 h prior to solvent (THF) removal.

entries 12 and 16) following solvent removal revealed the formation of a new  $\text{Mg}(\text{II})$ -species, although its identity remains unclear. It is suggested the dimeric framework dissociates in solution, affording a heteroleptic complex of the general formula  $\text{Mg}(\text{1,3})\text{L}$ , where L could be methoxy, lactyl or higher chain oligomers, as previously described by Jones and co-workers.<sup>123</sup> Consequently,  $[\text{Mg}(\text{1,3})]_2$  should strictly be regarded as pre-catalysts and this can likely be extended to the remaining  $\text{Zn}(\text{II})$ -complexes.

**PET degradation.** Presently, bio-based plastics account for *ca.* 1% of all processed plastics, with PLA accounting for just 13.9% of bioplastic production in 2019.<sup>126</sup> Consequently, our attention shifted to PET, a commercial polyester widely exploited in the packaging industry, which consumed 38% of plastics produced globally in 2015, with PET accounting for 22.6% of plastic use in the sector.<sup>13</sup> Glycolysis is the most widely used chemical recycling method for PET, characterised by cleavage of the ester bond *via* insertion of a glycol, commonly ethylene glycol (EG), to produce bis(2-hydroxyethyl) terephthalate (BHET) or higher alcohol derivatives. BHET can then be repolymerised to virgin PET or used as a precursor in the production of unsaturated polyester resins.<sup>127–131</sup> In light of this, preliminary work sought to apply  $[\text{Zn}(\text{1,3})]_2$  and  $[\text{Mg}(\text{1})]_2$  to the glycolysis of PET.  $[\text{Mg}(\text{3})]_2$  was not investigated due to insufficient yield. Typically, high temperatures (180–240 °C) and prolonged reaction times (0.5–8 h) in the presence of a transesterification catalyst, often a metal acetate, are required to achieve appreciable conversion. Whilst numerous metal acetate catalysts have been reported in the literature, zinc acetate is considered the benchmark.<sup>127,132</sup>

Consequently,  $\text{Zn}(\text{OAc})_2 \cdot 2\text{H}_2\text{O}$  (Sigma Aldrich) was chosen as an air-stable, commercially available reference. Additionally, high EG:PET ( $\geq 5:1$ ) are used to mediate the formation of higher chain oligomers, thus favouring the formation of BHET.<sup>127</sup> As such, a reaction temperature of 180 °C in the presence of 8 wt% catalyst and 27.5 equivalents of EG was chosen (Table 5). Two sources of PET were selected: 1. A carbonated drinks bottle ( $M_n \sim 40\,000 \text{ g mol}^{-1}$ ) and 2. Thin-films, representing waste from the manufacturing industry (Fig. 7).

Typically, a 6–12% reduction in  $Y_{\text{BHET}}$  (isolated yield) was observed on accounting for residual  $\text{H}_2\text{O}$  (1.3–3.5 equivalents)

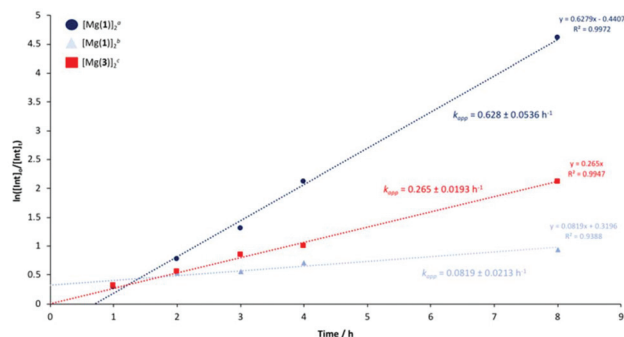


**Fig. 6** Pseudo-first-order logarithmic plot for the degradation of PLLA cup using  $[\text{Mg}(\text{1})]_2$  and  $[\text{Mg}(\text{3})]_2$  in THF at 80 °C. <sup>a</sup> $[\text{Mg}(\text{1})]_2 = 4 \text{ wt\% cat. loading}$  (0.29 mol% relative to ester linkages). <sup>b</sup> $[\text{Mg}(\text{1})]_2 = 8 \text{ wt\% cat. loading}$  (0.57 mol% relative to ester linkages). <sup>c</sup> $[\text{Mg}(\text{3})]_2 = 8 \text{ wt\% cat. loading}$  (0.53 mol% relative to ester linkages).



**Table 5** PET degradation into BHET using selected Zn(II)- and Mg(II)-catalen complexes at 180 °C

Catalyst	Time/h	<i>T</i> /°C	Cat. loading/wt%	EG/equiv.	<i>Y</i> <sub>BHET</sub> (wet) (g/%)	H <sub>2</sub> O/equiv.	Corrected <i>Y</i> <sub>BHET</sub> (%)
Ref	4	180	8	27.5	0.16 (48%)	2.0	42
	2 <sup>a</sup>	180	8	27.5	0.14 (42%)	2.1	37
[Zn(1)] <sub>2</sub>	4	180	8	27.5	0.20 (61%)	3.3	49
[Zn(3)] <sub>2</sub>	4	180	8	27.5	0.16 (48%)	1.3	44
[Mg(1)] <sub>2</sub>	3	180	8	27.5	0.20 (61%)	2.7	51
	0.75 <sup>a</sup>	180	8	27.5	0.14 (42%)	3.5	34
	3 <sup>b</sup>	180	8	27.5	0.18 (55%)	2.4	46

Reaction conditions: 0.25 g of carbonated drinks bottle (*M<sub>n</sub>* ~40 000 g mol<sup>-1</sup>), 27.5 equivalents of EG (relative to ester linkages), Ref: Zn(OAc)<sub>2</sub>·2H<sub>2</sub>O = 8 wt% cat. loading (0.02 g, 7 mol% relative to ester linkages), [Zn(1,3)]<sub>2</sub> = 8 wt% cat. loading (0.02 g, 1.3–1.4 mol% relative to ester linkages), [Mg(1)]<sub>2</sub> = 8 wt% cat. loading (0.02 g, 1.5 mol% relative to ester linkages). <sup>a</sup> PET thin-film (0.25 g). <sup>b</sup> PET (0.25 g, carbonated drinks bottle) + PVC (0.025 g, 10 wt%, Sigma Aldrich, *M<sub>n</sub>* ~22 000 g mol<sup>-1</sup>). N.B. *Y*<sub>BHET</sub> (wet) refers to the isolated yield of BHET recrystallised from deionised H<sub>2</sub>O, followed by drying at 90 °C for 3 h *in vacuo*. Residual H<sub>2</sub>O (equiv.) was determined *via* <sup>1</sup>H NMR (D<sub>6</sub>-DMSO) analysis. A corrected *Y*<sub>BHET</sub> is provided accounting for the complete removal of H<sub>2</sub>O.



**Fig. 7** (A) Metal mediated glycolysis of poly(ethylene terephthalate) (PET) into bis(2-hydroxyethyl) terephthalate (BHET) in the presence of ethylene glycol (EG), where R denotes the growth polymer chain. (B) Example of recycled product (BHET).

after drying, and thus cannot be considered absolute. Consequently, the discussion of *Y*<sub>BHET</sub> herein will refer to the corrected value. [Zn(1,3)]<sub>2</sub> exhibited comparable performance to the reference, achieving between 44–49% *Y*<sub>BHET</sub> within 4 h at 180 °C. Promisingly, [Mg(1)]<sub>2</sub> exhibited superior activity, ascertaining the highest *Y*<sub>BHET</sub> observed, achieving 51% within 3 h under analogous conditions. For this system, tolerance stability was successfully demonstrated in the presence of 10 wt% PVC, retaining comparable *Y*<sub>BHET</sub> (46%; Table 5, entry 7). PVC contamination as low as 100 ppm has previously been reported to adversely impact the quality of the final recycled product, owing to the production of acid catalysts that facilitate chain scission under melt reprocessing conditions (*T* = 160 °C) routinely employed in industry.<sup>127</sup> Thus, this result is particularly promising from an industrial perspective. Both [Mg(1)]<sub>2</sub> and Zn(OAc)<sub>2</sub>·2H<sub>2</sub>O exhibited superior activity on substituting the carbonated drinks bottle for thin-films, owing to superior sample dissolution. Remarkably, [Mg(1)]<sub>2</sub> achieved 34% *Y*<sub>BHET</sub> within 45 minutes, vastly outperforming the reference, which afforded comparable conversion within 2 h (*Y*<sub>BHET</sub> = 37%; Table 5, entry 2). Whilst reaction times reflect the time taken to achieve complete PET dissolution, indicative of reaction completion, *Y*<sub>BHET</sub> less than 50% were typically observed. It is possible the production of higher

chain oligomers is partly responsible.<sup>127–132</sup> In summary, [Zn(1,3)]<sub>2</sub> and [Mg(1)]<sub>2</sub> exhibited superior activity for PET glycolysis relative to Zn(OAc)<sub>2</sub>·2H<sub>2</sub>O, despite the wt% of the reference corresponding to a significantly higher zinc loading, highlighting the importance of structure-activity relationships.

## Conclusions

A range of dimeric Zn(II)- and Mg(II)-catalen complexes were prepared and fully characterised. The production of biocompatible atactic PLA in solution and under industrially preferred solvent-free conditions was demonstrated, typically observing good activity and *M<sub>n</sub>* control with a broad range of dispersities (*D* = 1.08–2.04). Mg(II)-Complexes were shown to facilitate the relatively mild methanolysis of PLA, achieving up to 64% conversion to Me-LA within 8 h at 80 °C in THF. Further kinetic analysis found [Mg(1,3)]<sub>2</sub> to have *k*<sub>app</sub> values of 0.628 ± 0.0536 {4 wt% cat. loading} and 0.265 ± 0.0193 h<sup>-1</sup> {8 wt% cat. loading} respectively. For [Mg(1)]<sub>2</sub>, increasing the catalyst loading to 8 wt% resulted in a statistically significant reduction in activity (0.0819 ± 0.0213 h<sup>-1</sup>), potentially evidencing catalyst aggregation, which appeared prevalent in the





Zn(II)-complexes. Preliminary work extended polymer scope to PET from various sources, demonstrating catalyst versatility.

## Conflicts of interest

The authors declare no conflict of interest.

## Acknowledgements

We wish to thank the EPSRC for funding and the University of Bath and MC<sup>2</sup> for use of their analysis facilities. We would like to thank the EPSRC for funding (EP/L016354/1) for a PhD studentship to J. P. and (EP/P016405/1) for P. M. We thank Avery Dennison for kindly providing waste PET thin-films used in this study.

## References

- 1 R. A. Sheldon and M. Norton, *Green Chem.*, 2020, **22**, 6310–6322.
- 2 PlasticsEurope, *Plastics – the Facts 2019. An Analysis of European Plastics Production, Demand and Waste Data*, 2019, [https://www.plasticseurope.org/application/files/9715/7129/9584/FINAL\\_web\\_version\\_Plastics\\_the\\_facts2019\\_14102019.pdf](https://www.plasticseurope.org/application/files/9715/7129/9584/FINAL_web_version_Plastics_the_facts2019_14102019.pdf), (Accessed: 13th October 2020).
- 3 J. Payne, P. McKeown and M. D. Jones, *Polym. Degrad. Stab.*, 2019, **165**, 170–181.
- 4 R. Geyer, J. R. Jambeck and K. L. Law, *Sci. Adv.*, 2017, **3**, 1–5.
- 5 R. C. Thompson, C. J. Moore, F. S. vom Saal and S. H. Swan, *Philos. Trans. R. Soc., B*, 2009, **364**, 2153–2166.
- 6 Y. Zhu, C. Romain and C. K. Williams, *Nature*, 2016, **540**, 354–362.
- 7 Ellen MacArthur Foundation, *The New Plastics Economy: Rethinking the future of plastics*, 2016, <https://www.ellenmacarthurfoundation.org/publications/the-new-plastics-economy-rethinking-the-future-of-plastics>, (Accessed: 7th January 2019).
- 8 J. R. Jambeck, R. Geyer, C. Wilcox, T. R. Siegler, M. Perryman, A. Andrady and R. Na, *Science*, 2015, **347**, 768–771.
- 9 L. Lebreton, B. Slat, F. Ferrari, B. Sainte-Rose, J. Aitken, R. Marthouse, S. Hajbane, S. Cunsolo, A. Schwarz, A. Levivier, K. Noble, P. Debeljak, H. Maral, R. Schoeneich-Argent, R. Brambini and J. Reisser, *Sci. Rep.*, 2018, **8**, 4666.
- 10 E. T. H. Vink, K. R. Rábago, D. A. Glassner, B. Springs, R. P. O'Connor, J. Kolstad and P. R. Gruber, *Macromol. Biosci.*, 2004, **4**, 551–564.
- 11 E. T. H. Vink, D. A. Glassner, J. Kolstad, R. J. Wooley and R. P. O'Connor, *Biotechnology*, 2007, **3**, 58–81.
- 12 J. Lunt, *Polym. Degrad. Stab.*, 1998, **59**, 145–152.
- 13 M. Rabnawaz, I. Wyman, R. Auras and S. Cheng, *Green Chem.*, 2017, **19**, 4737–4753.
- 14 R. E. Drumright, P. R. Gruber and D. E. Henton, *Adv. Mater.*, 2000, **12**, 1841–1846.
- 15 O. Dechy-Cabaret, B. Martin-Vaca and D. Bourissou, *Chem. Rev.*, 2004, **104**, 6147–6176.
- 16 R. H. Platel, L. M. Hodgson and C. K. Williams, *Polym. Rev.*, 2008, **48**, 11–63.
- 17 H. R. Kricheldorf, I. Kreiser-Saunders and A. Stricker, *Macromolecules*, 2000, **33**, 702–709.
- 18 N. Spassky, M. Wisniewski, C. Pluta and A. LeBorgne, *Macromol. Chem. Phys.*, 1996, **197**, 2627–2637.
- 19 Z. Y. Zhong, P. J. Dijkstra and J. Feijen, *Angew. Chem., Int. Ed.*, 2002, **41**, 4510–4513.
- 20 Z. Zhong, P. J. Dijkstra and J. Feijen, *J. Am. Chem. Soc.*, 2003, **125**, 11291–11298.
- 21 N. Nomura, R. Ishii, M. Akakura and K. Aoi, *J. Am. Chem. Soc.*, 2002, **124**, 5938–5939.
- 22 N. Nomura, R. Ishii, Y. Yamamoto and T. Kondo, *Chem. – Eur. J.*, 2007, **13**, 4433–4451.
- 23 H.-L. Chen, S. Dutta, P.-Y. Huang and C.-C. Lin, *Organometallics*, 2012, **31**, 2016–2025.
- 24 E. L. Whitelaw, G. Loraine, M. F. Mahon and M. D. Jones, *Dalton Trans.*, 2011, **40**, 11469–11473.
- 25 A. Pilone, K. Press, I. Goldberg, M. Kol, M. Mazzeo and M. Lamberti, *J. Am. Chem. Soc.*, 2014, **136**, 2940–2943.
- 26 P. McKeown, M. G. Davidson, G. Kociok-Köhn and M. D. Jones, *Chem. Commun.*, 2016, **52**, 10431–10434.
- 27 P. Hormnirun, E. L. Marshall, V. C. Gibson, A. J. P. White and D. J. Williams, *J. Am. Chem. Soc.*, 2004, **126**, 2688–2689.
- 28 P. Hormnirun, E. L. Marshall, V. C. Gibson, R. I. Pugh and A. J. P. White, *Proc. Natl. Acad. Sci. U. S. A.*, 2006, **103**, 15343–15348.
- 29 H. Du, A. H. Velders, P. J. Dijkstra, J. Sun, Z. Zhong, X. Chen and J. Feijen, *Chem. – Eur. J.*, 2009, **15**, 9836–9845.
- 30 J. Feijen, *Chem. – Eur. J.*, 2009, **15**, 9836–9845.
- 31 K. Press, I. Goldberg and M. Kol, *Angew. Chem., Int. Ed.*, 2015, **54**, 14858–14861.
- 32 R. Hador, A. Botta, V. Venditto, S. Lipstman, I. Goldberg and M. Kol, *Angew. Chem., Int. Ed.*, 2019, **58**, 14679–14685.
- 33 S. Gesslbauer, H. Cheek, A. J. P. White and C. Romain, *Dalton Trans.*, 2018, **47**, 10410–10414.
- 34 S. Gesslbauer, R. Savelle, Y. Chen, A. J. P. White and C. Romain, *ACS Catal.*, 2019, **9**, 7912–7920.
- 35 J. Payne, P. McKeown, G. Kociok-Köhn and M. D. Jones, *Chem. Commun.*, 2020, **56**, 7163–7166.
- 36 A. J. Chmura, M. G. Davidson, M. D. Jones, M. D. Lunn, M. F. Mahon, A. F. Johnson, P. Khunkamchoo, S. L. Roberts and S. S. F. Wong, *Macromolecules*, 2006, **39**, 7250–7257.
- 37 A. J. Chmura, M. G. Davidson, C. J. Frankis, M. D. Jones and M. D. Lunn, *Chem. Commun.*, 2008, 1293–1295.
- 38 A. J. Chmura, M. G. Davidson, C. J. Frankis, M. D. Jones and M. D. Lunn, *Chem. Commun.*, 2008, 1293–1295.
- 39 A. Sauer, A. Kapelski, C. Fliedel, S. Dagorne, M. Kol and J. Okuda, *Dalton Trans.*, 2013, **42**, 9007–9023.
- 40 E. Sergeeva, J. Kopilov, I. Goldberg and M. Kol, *Inorg. Chem.*, 2010, **49**, 3977–3979.





- 90 C. T. Bowmer, R. N. Hoofman, A. O. Hanstveit, P. W. M. Venderbosch and N. van der Hoeven, *Chemosphere*, 1998, **37**, 1317–1333.
- 91 C. S. M. Pereira, V. M. T. M. Silva and A. E. Rodrigues, *Green Chem.*, 2011, **13**, 2658–2671.
- 92 M. Dusselier, P. V. Wouwe, A. Dewaele, E. Makshina and B. F. Sels, *Energy Environ. Sci.*, 2013, **6**, 1415–1442.
- 93 Y. Fan, C. Zhou and X. Zhu, *Catal. Rev. Sci. Eng.*, 2009, **51**, 293–324.
- 94 V. Piemonte, S. Sabatini and F. Gironi, *J. Polym. Environ.*, 2013, **21**, 640–647.
- 95 F. M. Lamberti, L. A. Román-Ramírez, P. McKeown, M. D. Jones and J. Wood, *Processes*, 2020, **8**, 738.
- 96 H. Tsuji, T. Saeki, T. Tsukegi, H. Daimon and K. Fujie, *Polym. Degrad. Stab.*, 2008, **93**, 1956–1963.
- 97 V. Piemonte and F. Gironi, *J. Polym. Environ.*, 2013, **21**, 313–318.
- 98 P. Coszach, J.-C. Bogaert and J. Willocq, *US Pat*, 8431683B2, 2013.
- 99 C. F. VanNostrum, T. F. J. Veldhuis, G. W. Bos and W. E. Hennink, *Polymer*, 2004, **45**, 6779–6787.
- 100 H. Tsuji, H. Daimon and K. Fujie, *Biomacromolecules*, 2003, **4**, 835–840.
- 101 F. Codari, S. Lazzari, M. Soos, G. Storti, M. Morbidelli and D. Moscatelli, *Polym. Degrad. Stab.*, 2012, **97**, 2460–2466.
- 102 K. Odelius, A. Höglund, S. Kumar, M. Hakkarainen, A. K. Ghosh, N. Bhatnagar and A. C. Albertsson, *Biomacromolecules*, 2011, **12**, 1250–1258.
- 103 K. Hirao, Y. Nakatsuchi and H. Ohara, *Polym. Degrad. Stab.*, 2010, **95**, 925–928.
- 104 L. D. Brake, *US Pat*, 5264617, 1993.
- 105 X. Song, X. Zhang, H. Wang, F. Liu, S. Yu and S. Liu, *Polym. Degrad. Stab.*, 2013, **98**, 2760–2764.
- 106 X. Song, H. Wang, X. Zheng, F. Liu and S. Yu, *J. Appl. Polym. Sci.*, 2014, **131**, 40817–40822.
- 107 C. Fliedel, D. Vila-Viçosa, M. J. Calhorda, S. Dagorne and T. Avilés, *ChemCatChem*, 2014, **6**, 1357–1367.
- 108 E. L. Whitelaw, M. G. Davidson and M. D. Jones, *Chem. Commun.*, 2011, **47**, 10004–10006.
- 109 L. A. Román-Ramírez, P. McKeown, M. D. Jones and J. Wood, *ACS Catal.*, 2019, **9**, 409–416.
- 110 J. Payne, P. McKeown, M. F. Mahon, E. A. C. Emanuelsson and M. D. Jones, *Polym. Chem.*, 2020, **11**, 2381–2389.
- 111 R. Petrus, D. Bykowski and P. Sobota, *ACS Catal.*, 2016, **6**, 5222–5235.
- 112 F. A. Leibfarth, N. Moreno, A. P. Hawker and J. D. Shand, *J. Polym. Sci., Part A: Polym. Chem.*, 2012, **50**, 4814–4822.
- 113 F. Nederberg, E. F. Connor, T. Glausser and J. L. Hedrick, *Chem. Commun.*, 2001, 2066–2067.
- 114 P. McKeown, M. Kamran, M. G. Davidson, M. D. Jones, L. A. Román-Ramírez and J. Wood, *Green Chem.*, 2020, **22**, 3721–3726.
- 115 A. C. Sánchez and R. S. Collinson, *Eur. Polym. J.*, 2011, **47**, 1970–1976.
- 116 S. Westhues, J. Idel and J. Klankermayer, *Sci. Adv.*, 2018, 1–9.
- 117 E. M. Krall, T. W. Klein, R. J. Andersen, A. J. Nett, R. W. Glasgow, D. S. Reader, B. C. Dauphinais, S. P. Mc Ilrath, A. A. Fischer, M. J. Carney, D. J. Hudson and N. J. Robertson, *Chem. Commun.*, 2014, **50**, 4884–4887.
- 118 T.-O. Kindler, C. Alberti, E. Fedorenko, N. Santangelo and S. Enthaler, *ChemistryOpen*, 2020, **9**, 401–404.
- 119 L. Monsigny, J.-C. Berthet and T. Cantat, *ACS Sustainable Chem. Eng.*, 2018, **6**, 10481–10488.
- 120 H. Liu, X. Song, F. Liu, S. Liu and S. Yu, *J. Polym. Res.*, 2015, **22**, 135–141.
- 121 C. Alberti, N. Damps, R. R. R. Meißner, M. Hofmann, D. Rijono and S. Enthaler, *Adv. Sustainable Syst.*, 2020, **4**, 1900081.
- 122 M. Hofmann, C. Alberti, F. Scheliga, R. R. R. Meißner and S. Enthaler, *Polym. Chem.*, 2020, **11**, 2625–2629.
- 123 P. McKeown, L. A. Román-Ramírez, S. Bates, J. Wood and M. D. Jones, *ChemSusChem*, 2019, **12**, 5233–5238.
- 124 A. J. Hunt, T. J. Farmer and J. H. Clark, *Chapter 1 Elemental Sustainability and the Importance of Scarce Element Recovery*, in *Element Recovery and Sustainability*, ed. A. Hunt, RSC, 2013, ch. 1, pp. 1–28.
- 125 ACS, *12 Principles of Green Chemistry*, <https://www.acs.org/content/acs/en/greenchemistry/principles/12-principles-of-green-chemistry.html>, (Accessed: 19th October 2020).
- 126 European Bioplastics, Facts and Figures, [https://docs.european-bioplastics.org/publications/EUBP\\_Facts\\_and\\_figures.pdf](https://docs.european-bioplastics.org/publications/EUBP_Facts_and_figures.pdf), (Accessed: 20th October 2020).
- 127 F. M. Lamberti, L. A. Román-Ramírez and J. Wood, *J. Polym. Environ.*, 2020, **28**, 2551–2571.
- 128 V. Sinha, M. R. Patel and J. V. Patel, *J. Polym. Environ.*, 2010, **18**, 8–25.
- 129 S. M. Al-Salem, P. Lettieri and J. Baeyens, *Waste Manage.*, 2009, **29**, 2625–2643.
- 130 G. P. Karayannidis and D. S. Achilias, *Macromol. Mater. Eng.*, 2007, **292**, 128–146.
- 131 D. Paszun and T. Szychaj, *Ind. Eng. Chem. Res.*, 1997, **36**, 1373–1383.
- 132 K. R. Della Chiaie, F. R. McMahon, E. J. Williams, M. J. Price and A. P. Dove, *Polym. Chem.*, 2020, **11**, 1450–1453.

